

Research on Intelligent Fault Identification Technology of Wind Turbine Supported by Fault Knowledge Base

*Fei Chen, **Zhongguang Fu, ***Zhiling Yang

*School of Energy, Power and Mechanical Engineering, North China Electric Power University, Beijing, China, 2 Beinong Rd., Changping District, Beijing 102206, (chenfei@ncepu.edu.cn)

** School of Energy, Power and Mechanical Engineering, North China Electric Power University, Beijing, China, 2 Beinong Rd., Changping District, Beijing 102206, (fzg@ncepu.edu.cn)

*** School of Energy, Power and Mechanical Engineering, North China Electric Power University, Beijing, China, 2 Beinong Rd., Changping District, Beijing 102206,

(yzhil@ncepu.edu.cn)

Abstract

Wind power companies are increasingly introducing fault diagnosis technologies, however, the full use of these technologies mainly depends on expert experience. This paper puts forward a fault identification method for the intelligent fault identification of wind turbine based on fault knowledge base. The model uses principal component analysis to integrate the eigenvalues of vibration and SCADA signals, and then takes the existing fault sample with the highest matching rate in the wind farm fault knowledge base as the input to train the least squares support vector regression algorithm model optimized by particle swarm optimization. The matching rates of fault samples in the fault knowledge base are updated after each diagnosis. Finally, the measured data of the wind farm are used to verify the effect of the model. It is proved that, if the fault samples are sufficiently trained, this method can accurately diagnose the existing faults from the fault base.

Key words

Intelligent fault identification; knowledge base; data fusion; wind turbine

1. Introduction

As the main equipment of wind farm, wind turbine takes up 74-82% of the total investment on wind farm. What is worse, the wind turbine is also the major contributor to the operating cost of the wind farm because of its high failure rate in the poor operating environment and expensive maintenance cost. Suffice it to say that the economic benefits of wind farm hinge on the reduction of wind power turbine maintenance cost. Thus, wind power companies are increasingly introducing technologies such as condition monitoring, fault diagnosis and condition maintenance. The problem is most of the condition monitoring and fault diagnosis systems on the market only support achieve data acquisition and signal processing functions. For complex functions like fault diagnosis, positioning and prediction functions, experienced fault diagnosis experts are needed to make judgements based on the frequency domain analysis of the collected signals. In the lack of expertise, field maintenance staff often fail to make full use of the software based on expert experience.

Scientific workers at home and abroad have carried out some research on intelligent diagnosis of wind turbine. The representative works are listed below. Peng Huadong [1] presents a flow chart of wind turbine fault diagnosis model based on BP neural network and the corresponding software function module [1]. Su (2015) pointed out the main functions of online remote fault diagnosis system of wind turbine [2]. Roozbeh (2013) applied Dynamic Weighting Ensembles Algorithm in fault identification of doubly-fed asynchronous generators [3]. Adel (2014) used Gaussian acyclic graphical models and Lasso to estimate the fault of variable pitch system [4]. Gu (2016) preprocessed the original vibration signal by the step ratio sampling method and the dimension-factor analysis, sets up the early fault identification model of the wind turbine gearbox based on the Mahalanobis distance, and adopts the MLR-improved multiple outlier monitoring method to achieve the early fault diagnosis of fan gearbox [5]. For the purpose of determining the relationship between the transmission efficiency, temperature and speed signal of the wind turbine gearbox, Qiu (2014) established a wind turbine transmission chain model in consideration of the heat transfer mechanism in the gearbox lubrication system, thereby offering useful information for the design and optimization of the lubrication system [6]. Through comparison between the gearbox and generator simulation results and the SCADA data, Qiu (2016) proved the validity of the diagnostic method in that it can identify some failure modes difficult to be identified by vibration analysis [7]. Hasmat (2015) employed Simulink, FAST and TurbSim to establish the permanent magnet synchronous wind turbine simulation model, obtains the intrinsic mode frequency of signal through the EMD decomposition of the stator current

outputs of the model under normal operation and various imbalance faults, and imports the decomposition results to the probabilistic neural network to identify the imbalance faults of the wind turbine [8]. Alkhadafe (2016) chooses Taguchi orthogonal array and eigenvalue automatic selection method to optimize the selective sensor and signal processing algorithms, and verifies the effectiveness of the two algorithms by applying them in the diagnosis of three damage degrees of helical gear of single stage gearbox [9-10]. To improve the speed of big data processing of fault diagnosis and early warning methods without sacrificing the accuracy.

It can be seen from the above research that intelligent diagnosis is the mainstream approach to diagnose the faults of vibration signals or SCADA signals on key components of wind turbine, such as gearbox and generator. Against this backdrop, this paper puts forward a fault identification method for the intelligent fault identification of wind turbine based on fault knowledge base. The model is constructed as follows: use principal component analysis to integrate the eigenvalues of vibration and SCADA signals, and then take the existing fault sample with the highest matching rate in the wind farm fault knowledge base as the input to train the least squares support vector regression algorithm and gravitational neural network algorithm.

2. Data collection and fusion

2.1 SCADA data and vibration data

The supervisory control and data acquisition (SCADA) system of wind turbine data can collect and transmit the status parameters of wind turbine, including wind wheel speed, generator speed, generator coil temperature, the temperatures of the front and rear bearings of the generator, gearbox oil temperature, the temperatures of the front and rear bearings of the gearbox, hydraulic system oil temperature, oil pressure, oil level, engine room vibration, cable torsion, and engine room temperature. Nevertheless, the SCADA information on temperatures and oil pressures are often insufficient to determine the specific type and location of faults on gearbox and some other key parts of the wind turbine.

This paper provides a wind turbine condition monitoring system capable of collecting the vibration information and SCADA data of the wind turbine. (Figure 1) The system consists of onboard data acquisition system and wind farm data server. The onboard data acquisition system contains a controller, a transmission chain vibration data acquisition module, a sensor, a data processing module, a data storage module, a SCADA data acquisition module and a data communication module. Among them, the SCADA data acquisition module reads data from wind

turbine main PLC control, and the data communication module is connected to the wind farm data server.

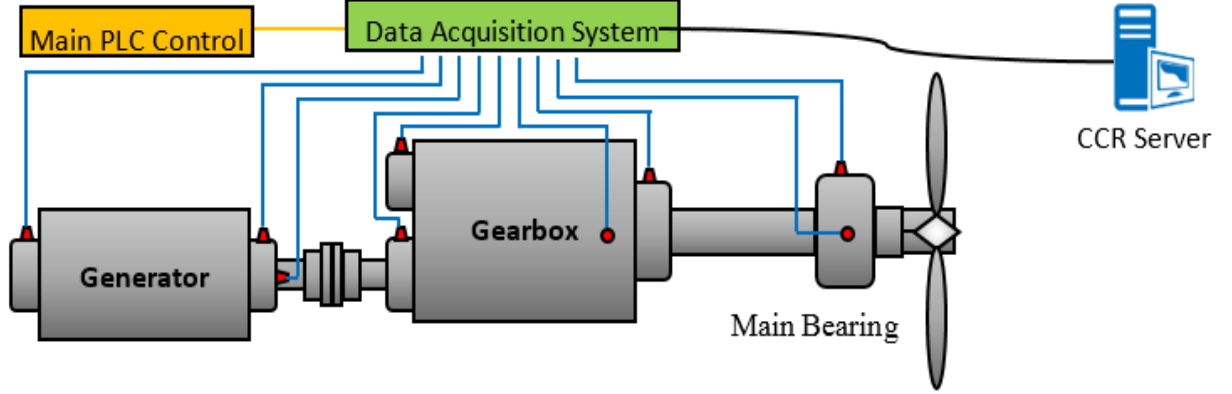


Fig. 1 Data acquisition system

2.2 Data feature extraction

The raw data collected by the data acquisition system cannot be used directly for fault diagnosis. It is necessary to choose proper characteristic parameters, and extract the features of the original data. The characteristic parameters are described as follows:

1) The absolute mean X_{AM} and the range X_R . Related to the signal amplitude, the two parameters are sensitive to the vibration energy, and their values increase as the fault develops.

The values are calculated by the following formula:

$$X_{AM} = \frac{\sum_{i=1}^n |x_i|}{n} \quad (1)$$

$$X_R = X_{max} - X_{min} \quad (2)$$

Where x_i is the value of the i -th data in the data sequence, X_{max} is the maximum value of the data sequence, and X_{min} is the minimum value of the data sequence.

2) The waveform factor X_{SF} . The parameter is sensitive to the slight fluctuation of the shape of the vibration signal. Its value is calculated by the following formula:

$$X_{SF} = \frac{\sqrt{n \sum_{i=1}^n x_i^2}}{\sum_{i=1}^n |x_i|} \quad (3)$$

3) Kurtosis X_K . The parameter is sensitive to the impact signal response. Its value is calculated by the following formula:

$$X_K = \frac{1}{n} \sum_{i=1}^n \frac{(x_i - \bar{x})^4}{\sigma^4} \quad (4)$$

Where \bar{x} is the average of the data sequence and σ is the standard deviation of the data sequence.

4) Frequency centroid BFS. The parameter is sensitive to the spectral variation of the vibration signal. Its value is calculated by the following formula:

$$\text{BSF} = \frac{\sum_{i=1}^m f_i s(f_i)}{\sum_{i=1}^m s(f_i)} \quad (5)$$

Where $s(f)$ is the power spectrum of the signal.

5) Wavelet packet spectral entropy PSE(k). The parameter is sensitive to the variation in information quantity obtained by wavelet packet decomposition of the vibration signal. Its value is calculated by the following formula:

$$\text{PSE}(k) = \sum_{i=1}^l [P_k(i) \log P_k(i)] \quad (6)$$

Where p_k is the k -th wavelet packet sequence obtained by wavelet packet decomposition of the signal.

2.3 Data fusion

According to its role in the fault diagnosis algorithm, the data fusion can be divided into: data level fusion, feature level fusion and decision level fusion. (Figure 2)

In data level fusion, the raw data from various sensors are summarized and analyzed directly on the layer of the acquired raw data. In feature level fusion, the features extracted from the data level are associated and classified, and the system condition is judged by a certain fusion rule. In decision level fusion, the preliminary conclusions of the fault diagnosis on sub-systems are associated into the decision level judgement to yield the final joint inference results.

In this paper, the principal component analysis is used to perform feature-level data fusion [11]. The method reassembles the numerous partially relevant parameters (e.g. n characteristic parameters) into a group of new, irrelevant composite indices to replace the original indices. The

data fusion process removes the redundancy in the characteristic parameters, reduces the original feature dimensions, and thereby generates the feature-reduced composite indices.

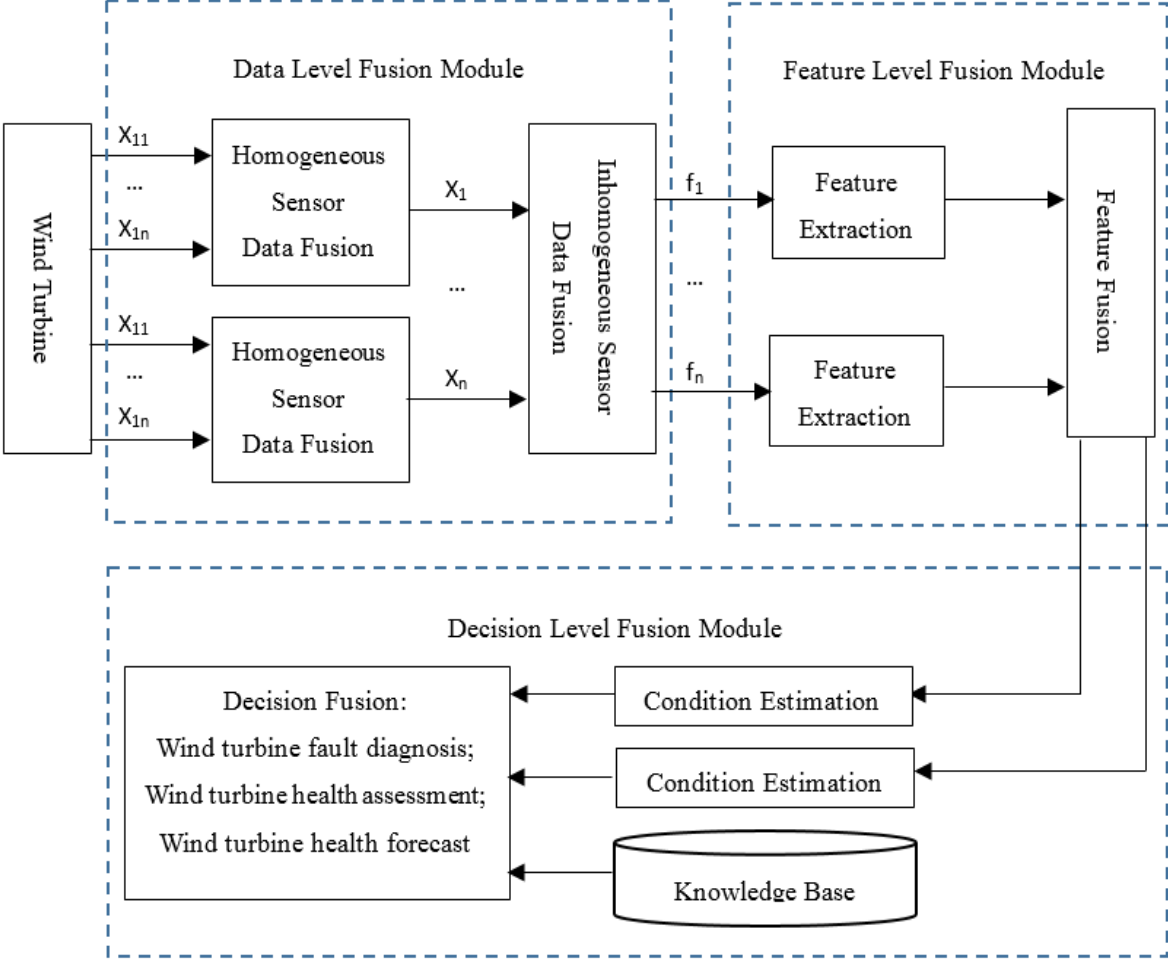


Fig. 2 The role of data fusion in fault diagnosis algorithm

This paper extracts a total of 12 characteristic parameters through a 3-layer wavelet packet decomposition of vibration data samples. The parameters include 8 wavelet packet energy spectral entropies, 3 time domain characteristic parameters (absolute mean, waveform factor, kurtosis) and 1 frequency domain characteristic (frequency centroid). The 12 characteristic parameters, coupled with the 2 time field eigenvalues (absolute mean and range) extracted from the SCADA information, constitute a 14-dimensional eigenvector of the condition of wind turbine. Finally, the 14-dimensional eigenvector receives data fusion by principal component analysis.

3. Fault knowledge base

The known fault types and the corresponding characteristic parameter samples must be imported to the fault knowledge base before the intelligent fault diagnosis of wind turbine. Any new fault should be compared with the characteristic parameter samples of the known faults in the fault knowledge base by the intelligent diagnosis algorithm, and the type of the new fault should be determined based on the successful matching rate.



Fig. 3 The structure of fault knowledge base

As time goes, there will be a gradual increase in the training samples of the same fault taken from different wind turbines in the fault knowledge base. This gives rise to the question of how to choose proper training samples. The answer is to take the fault data of the wind turbine with high successful matching rate as the training samples of the intelligent diagnosis. Figures 3 & 4 illustrate the structure of fault knowledge base and the matching rate update algorithm, respectively.

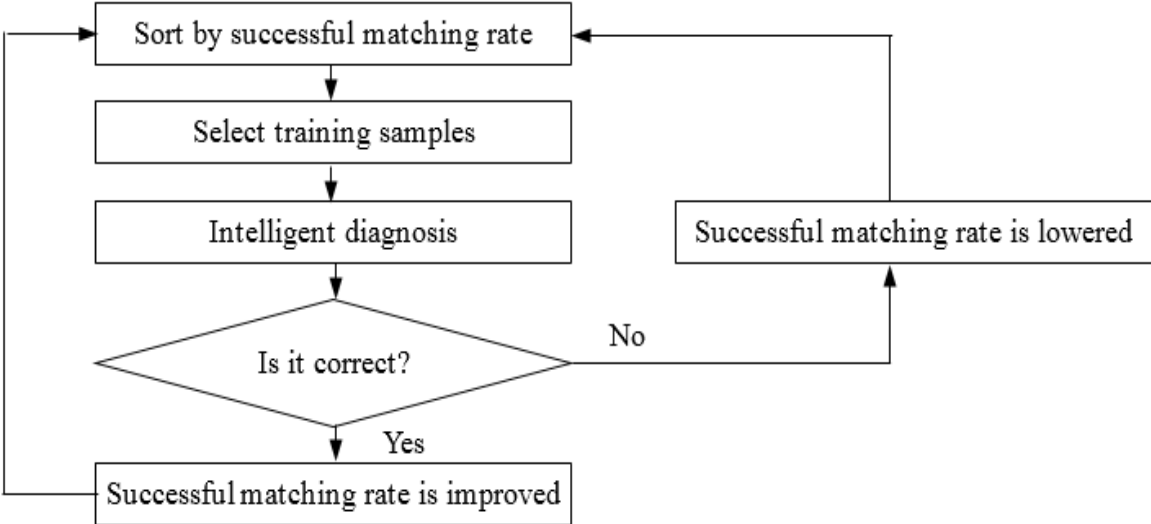


Fig. 4 Matching rate update algorithm

The base records every type of fault occurred to each component, and saves the historical conditions of each fault type monitored at different times and of different wind turbines under each fault type of each component. These monitoring data are called training samples, each of which carries the attribute of successful matching rate. The matching rate update algorithm goes as follows:

- 1) When a new fault occurs, the training samples are sorted by successful matching rate;
- 2) All samples with the highest successful matching rates are selected to form the training samples for this diagnosis, together with the corresponding fault types. For example, sample A1 is selected for the fault type A, and sample B4 is selected for fault type B;
- 3) The intelligent diagnostic model trained by the sample is applied to this fault diagnosis;
- 4) The diagnostic results indicate which of the fault types in the fault knowledge base the new fault belongs to (e.g. fault type A). The judgment is verified by the maintenance personnel.
- 5) Update the successful matching rate. If the judgment is correct, the successful matching rate of the sample A1, corresponding to the fault type A, and the inverse is true.

4. Fault knowledge base

Supported by the fault knowledge base, the training samples are used to train the intelligent fault diagnosis model. In this paper, the firefly algorithm is used to optimize the least squares support vector regression algorithm. The algorithms are described as follows.

4.1 Least squares support vector regression algorithm

With multidimensional vector as the input and one-dimensional vector as the output, the least squares support vector regression (LS-SVR) is, in essence, a nonlinear mapping from original space to the high dimensional space and the construction of the optimal linear regression function. In the principle of structural risk minimization, the dot product operation in high dimensional feature space is replaced by the kernel function in the original space. In this way, the solution to the nonlinear estimation function is transformed into that to the linear estimation function in the high-dimensional feature space [12].

Suppose the training set has m samples, $x_i \in R^m$ is the input data and $y_i \in R$ is the output data. The problem is optimized by LS-SVR into [13]:

$$\min(J(w, \xi)) = \frac{1}{2}w^T w + \frac{C}{2} \sum_{i=1}^l \xi^2 \quad (7)$$

$$\text{s.t. } y_i = w^T \varphi(x_i) + b + \xi_i \quad (i = 1, 2, \dots, l) \quad (8)$$

Where J is the loss function; w is the weight vector; ξ_i is the empirical error; b is the offset amount; C is the penalty coefficient; $\varphi(\mathbf{x})$ is the non-linear mapping of the input data to the high-dimensional feature space.

The Lagrange polynomial of the dual problem is:

$$L(w, b, \xi, \alpha) = J(w, \xi) - \sum_{i=1}^l \alpha_i [w^T \varphi(x_i) + b + \xi_i - y_i] \quad (9)$$

Where α_i is a Lagrange multiplier.

By the KKT condition, seek partial derivative of w , ξ_i , b and α_i , respectively, and make it equal to 0. Eliminate w and ξ_i to get:

$$\begin{bmatrix} 0 & I^T \\ I & \Omega + C^{-1}E \end{bmatrix} \begin{bmatrix} b \\ \alpha \end{bmatrix} = \begin{bmatrix} 0 \\ y \end{bmatrix} \quad (10)$$

Where $I = [1, 1, \dots, 1]^T$; $\alpha = [\alpha_1, \alpha_2, \dots, \alpha_l]^T$; $y = [y_1, y_2, \dots, y_l]^T$; E is a $l \times l$ dimensional unit matrix; $\Omega_{ij} = \varphi(x_i) \varphi(x_j) = K(x_i, x_j)$ is a kernel function that satisfies the Mercer condition.

Select the following radial basis function kernel:

$$K(x_i, x_j) = \exp\left(-\frac{\|x_i - x_j\|^2}{2\sigma^2}\right) \quad (11)$$

Where σ is the width parameter of the kernel function; $\|x_i - x_j\|$ is the 2-norm.

The following LS-SVR decision function is obtained as:

$$f(x) = \sum_{i=1}^l \alpha_i \exp\left(-\frac{\|x_i - x_j\|^2}{2\sigma^2}\right) + b \quad (12)$$

The accuracy of LS-SVR model is determined by the penalty coefficient C and the kernel parameter σ . To avoid the blindness of manual selection, the author relies on the superior global search capability of the Particle Swarm Optimization (PSO) to find the optimal combination of penalty factor C and kernel parameter σ .

4.2 PSO algorithm

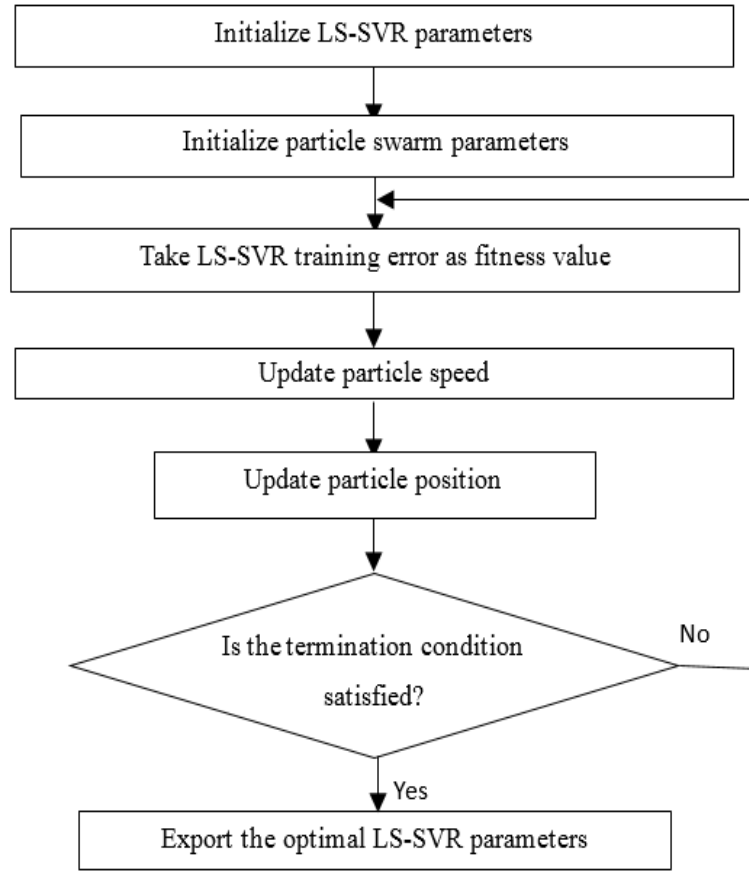


Fig. 5 Flowchart of PSO-optimized LS-SVR algorithm

In the PSO algorithm, the potential solution of the optimization problem is regarded as a particle in the n -dimensional search space. A number of randomly distributed initial particles are moving at a certain speed in the search space. The speed depends on their own inertia, optimal position and the optimal position of the population. To put it in another way: In an n -dimensional search space, there are m examples making up population $\mathbf{x} = (x_1, x_2, \dots, x_m)^T$. For the i -th particle, the position is $\mathbf{x}_i = (x_{i1}, x_{i2}, \dots, x_{in})^T$, the speed is $\mathbf{v}_i = (v_{i1}, v_{i2}, \dots, v_{in})^T$, and the current optimal position is $\mathbf{p}_i = (p_{i1}, p_{i2}, \dots, p_{in})^T$ for the individual. The current optimal position of the population is $\mathbf{g}_i = (g_1, g_2, \dots, g_n)^T$. The speed and position of each particle are updated according to the following formulas:

$$\mathbf{v}_{i,d}^{k+1} = \mathbf{v}_{i,d}^k + \text{rand}(\)(\mathbf{p}_{i,d}^k - \mathbf{x}_{i,d}^k) + \text{rand}(\)(\mathbf{g}_d^k - \mathbf{x}_{i,d}^k) \quad (13)$$

$$x_{i,d}^{k+1} = x_{i,d}^k + v_{i,d}^{k+1} \quad (14)$$

Where $\text{rand}(\)$ is a random number in $(0, 1)$; $v_{i,d}^k$ and $x_{i,d}^k$ are the speed and position of particle i in the d -th dimension in the k -th iteration; $p_{i,d}^k$ is the optimal position of particle i in the d -th dimension in the k -th iteration; g_d^k is the optimal position of the population in the d -th dimension in the k -th iteration.

Figure 5 is the flow chart of PSO-optimized LS-SVR algorithm.

5. Application and analysis

5.1 Application case data and algorithm initial setting

The monitoring data of a wind farm in Jilin Province are used to verify the proposed algorithm. The data are collected from four 1.5MW wind turbines. The first wind turbine has worn gear at the end of high speed shaft; the second has fractured gear at the end of high speed shaft; the third has loosened bearing at the end of high speed shaft; the fourth one is operating in the normal condition. The four wind turbines are diagnosed separately with the intelligent diagnosis method supported by the fault base.

In LS-SVR, the penalty coefficient C falls in the range of $[1, 1000]$ and the kernel parameter σ falls in the range of $[0.01, 10]$. In the PSO algorithm, the number of particles is set to 100, and the initial position and the speed are random numbers. The author uses the PSO algorithm to obtain the optimal combination of the penalty coefficient and kernel parameter of LS-SVR model, and substitutes the optimal combination into the model to diagnose the faults of the gearboxes of the wind turbines.

5.2 Fault diagnosis example

As mentioned above, for the training samples automatically organized by the fault knowledge base, 12 characteristic parameters are extracted from the vibration signal, including 8 wavelet packet energy spectral entropies, 3 time domain characteristic parameters (absolute mean, waveform factor, kurtosis) and 1 frequency domain characteristic (frequency centroid); Besides, 2 time domain eigenvalues (absolute mean and range) are extracted from the information on rear bearing temperature of the gearbox out of the SCADA information. The resulting 14-dimensional eigenvector of wind turbine conditions receives data fusion by the principal component analysis. Table 1 presents some of the extracted characteristic parameters. Given the limited space

available, the table only listed 1 of the 8 wavelet packet energy spectral entropies. Table 2 displays the input training samples obtained through the principal component analysis. The principal component analysis threshold is 0.95. The PSO-optimized LS-SVR model is used to optimize and train the input parameters. In this way, the intelligent diagnosis model is constructed with $C = 150.4668$ and $\sigma = 0.1532$.

The measured data of the four different wind turbines are processed with the above data processing method and imported to the above-mentioned trained intelligent diagnosis model. The diagnosis results and errors are shown in Table 3.

Table 1. Some of the extracted characteristic parameters

Healthy conditions	Vibration data					SCADA data	
	Absolute mean	Waveform factor	Kurtosis	Frequency centroid	Energy spectral entropy of wavelet packet	Absolute mean	Range
Normal	0.0541	1.1905	2.2247	1245.8413	6.7984	63.6606	0.8200
	0.0903	1.2305	2.6851	1413.3221	6.7203	66.2157	3.4000
	0.2040	1.2451	2.8301	1445.3789	6.9342	67.3535	1.8000
Worn gear at the end of high speed shaft	7.0757	1.3657	2.5418	571.3286	6.9615	63.7185	0.4800
	14.8514	1.3155	2.2570	943.0045	7.1044	66.3377	1.4600
	19.5166	1.3331	2.4506	781.7550	7.0390	63.9918	2.9300
Fractured gear at the end of high speed shaft	25.7708	1.4294	7.3398	1303.1139	7.5145	62.2949	3.0400
	35.0609	1.3996	7.6343	1344.1135	7.3756	64.2483	0.5800
	41.5687	1.5110	8.9068	1378.7435	7.3503	64.7028	2.5000
Loosened bearing at the end of high speed shaft	0.3447	1.2849	3.7505	1410.6124	6.1864	73.4782	1.3300
	0.3719	1.2727	3.4801	1411.0069	6.3094	75.4625	1.3800
	0.4207	1.2985	3.9361	1368.3230	6.0836	79.9989	3.0500

Table 2. Some of the training samples after data fusion

Healthy conditions	Condition code	Main component 1	Main component 2	Main component 3	Main component 4	Main component 5	Main component 6
Normal	1	22.143	-48.823	-97.409	-35.176	-146.949	53.173
		20.940	-47.015	-93.260	-35.116	-141.151	50.232

		17.471	-41.985	-81.023	-30.960	-121.798	41.486
Worn gear at the end of high speed shaft	2	-44.275	67.895	153.946	57.169	244.314	-102.512
		-38.494	58.975	133.201	51.146	211.003	-88.075
		-36.259	53.483	125.165	46.439	198.699	-84.306
Fractured gear at the end of high speed shaft	3	18.787	3.436	-51.824	-21.730	-84.400	53.882
		14.225	8.017	-38.142	-15.557	-64.187	45.649
		19.961	4.7139	-56.815	-24.077	-91.877	56.293
Loosened bearing at the end of high speed shaft	4	11.390	-29.602	-33.624	-11.738	-53.400	14.797
		10.456	-27.410	-28.265	-8.5266	-44.061	10.821
		14.411	-33.468	-43.557	-14.770	-68.708	21.610

Table 3. Fault diagnosis results and errors

Test no.	Actual condition	Target output	Actual output	Error
1	Normal	1	1.0703	0.0703
2	Worn gear at the end of high speed shaft	2	2.0842	0.0842
3	Fractured gear at the end of high speed shaft	3	2.9445	-0.0555
4	Loosened bearing at the end of high speed shaft	4	3.8698	-0.1302

6. Conclusion

This paper offers a complete fault diagnosis method of wind turbine supported by fault knowledge base:

1) The training samples of the intelligent fault diagnosis model are the samples with the highest successful matching rate in the fault knowledge base.

2) According to the vibration data and SCADA data in the training samples, the main feature analysis method is used to fuse the characteristic parameters of conditions.

3) The integrated composite indices are imported to the intelligent diagnosis model, and the PSO-optimized LS-SVR algorithm serves as the intelligent fault diagnosis method for the wind turbine.

The proposed method achieves excellent identification effect when it is applied to the fault diagnosis at the high-speed shaft end of wind turbines demonstrates. It provides a promising

solution to the problem that wind farm maintenance personnel do not have the expertise required for correctly reading the monitoring information of wind turbine.

References

1. H.D. Peng, X.Q. Chen, M. Ren, D.Y. Yang, M. Dong, Intelligent Fault Diagnosis Technology and System for Wind Turbines, 2011, *Advances of Power System and Hydroelectric Engineering*, vol. 27, no. 2, pp. 61-66.
2. W.D Su, Application of Online Remote Fault Diagnosis System for Wind Turbine, 2015, *Electric Safety Technology*, vol. 17, no.5, pp. 63-65.
3. R. Razavi-Far, M. Kinnaert, A Multiple Observers and Dynamic Weighting Ensembles Scheme for Diagnosing New Class Faults in Wind Turbines, 2013, *Control Engineering Practice*, vol. 21, no. 9, pp. 1165–1177.
4. A. Aloraini, M. Sayed-Mouchaweh, Graphical Model Based Approach for Fault Diagnosis of Wind Turbines, 2014, *International Conference on Machine Learning and Applications*, pp. 614-619.
5. Y.J. Gu, Z.W. Jia, R. Wang, Y.T. Ren, Early Fault Diagnosis for Wind Turbine Gearbox Based on Improved Multivariate Outlier Detection, 2016, *China Mechanical Engineering*, vol. 27, no. 14, pp. 1905-1910.
6. Y.N. Qiu, J. Sun, M. Cao, H. Wang, Model Based Wind Turbine Gearbox Fault Detection on SCADA Data, 2014, *IET Renewable Power Generation Conference*, pp. 1-5.
7. Y.N. Qiu, Y.H. Feng, J. Sun, H. Wang, Applying Thermophysics for Wind Turbine Drivetrain Fault Diagnosis Using SCADA Data, 2016, *IET Renewable Power Generation*, vol. 10, no. 5, pp. 661-668.
8. H. Malik, S. Mishra, Application of Probabilistic Neural Network in Fault Diagnosis of Wind Turbine Using FAST, TurbSim and Simulink, 2015, *Procedia Computer Science*, vol. 58, pp. 186-193.
9. H. Alkhadafe, A. Al-Habaibeh, A. Lotfi, Condition Monitoring of Helical Gears Using Automated Selection of Features and Sensors, 2016, *Measurement*, vol. 93, pp. 164–177.
10. S.M. Zhang, D. Mao, B.Y. Wang, Application of Big Data Processing Technology in Fault Diagnosis and Early Warning of Wind Turbine Gearbox, 2016, *Automation of Electric Power Systems*, vol. 40, no.14, pp. 129-134.
11. Q. Wu, H.N. Cai, L.F. Huang, Feature-level Fusion Fault Diagnosis Based on PCA, 2011, *Computer Science*, vol. 38, no. 1, pp. 268-270.

12. Q. Xu, Y.Q. Liu, D. Tian, J.H. Zhang, Q. Long, Fault Diagnosis of Rolling Bearings Using Least Square Support Vector Regression Based on Glowworm Swarm Optimization Algorithm, 2014, Journal of Vibration and Shock, vol. 33, no. 10, pp. 8-12.
13. H.Q. Wei, Z.M. Niu, W.H. Jiang, Y.L. Ye, Application of LSSVR Optimized by Adaptive Genetic Algorithm at Modeling Igniting Temperature of Pulverized-Coal, 2011, Journal of Combustion Science and Technology, vol. 17, no. 3, pp. 191-195.